Method to solve the limitations in drawing external rays of the Mandelbrot set

M Romera[1], G Pastor[1], A B Orue[1], A Martin[1], M F Danca[2,3,*] and F Montoya[1]

[1] Information Security Institute, CSIC, Serrano 144, 28006 Madrid, Spain,
[2] Dept. of Mathematics and Computer Science "Avram Iancu" University, Ilie Măcelaru 1A, 400380 Cluj-Napoca, România,
[3] Romanian Institute of Science and Technology, Cireşilor 29, 400487 Cluj-Napoca, România,

Abstract

The external rays of the Mandelbrot set are a valuable graphic tool in order to study this set. They are drawn using computer programs starting from the Böttcher coordinate. However, the drawing of an external ray cannot be completed because it reaches a point from which the drawing tool cannot continue drawing. This point is influenced by the resolution of the standard for floating-point computation used by the drawing program. The IEEE 754 Standard for Floating-Point Arithmetic is the most widely-used standard for floating-point computation, and we analyze the possibilities of the quadruple 128 bits format of the current IEEE 754-2008 Standard in order to draw external rays. When the drawing is not possible, due to a lack of resolution of this Standard, we introduce a method to draw external rays based on the escape lines and Bézier curves.

Mathematics Subject Classification: 37F45, 68M15

1. Introduction

As is well known, the Mandelbrot set can be defined by $\mathcal{M} = \left\{ c \in \mathbb{C} : f_c^{\circ k}(0) \nrightarrow \infty \text{ as } k \to \infty \right\}$, where $f_c^{\circ k}(0)$ is the k-iteration of the parameter-dependent quadratic function $f_c(z) = z^2 + c$ (z and c complex) from the initial value $z_0 = 0$ (the critical point).

In the 1980's, Douady and Hubbard published the external arguments theory of the Mandelbrot set [1,2]. Douady popularized this theory [3] by considering a capacitor made of a

*Corresponding author: danca@rist.ro

hollow metallic cylinder with great diameter, whose axis was an aluminum bar shaped in such a way that its cross-section was $\mathcal{M}$. If the capacitor is connected to a battery appears an electric field between the cylinder and $\mathcal{M}$, with equipotential lines and field lines. The field lines are the external rays of Douady and Hubbard, and the numbers associated with the external rays (between 0 and 1) are the external arguments of Douady and Hubbard. This electric field is extremely complicated because is generated in a capacitor where one of their plates is a fractal. For this reason, mathematicians and engineers may be interested in that study. The external rays and its external arguments identify graphically and numerically all the periodic components and Misiurewicz points (preperiodic points) of $\mathcal{M}$ and, therefore, the drawing of the external rays is important to study the ordering of $\mathcal{M}$.

The computer programs to draw external rays of the Mandelbrot set use the Böttcher coordinate $\Phi(c)$ given by [4]:

$$\Phi(c) = c \prod_{n=1}^{\infty} \left[1 + \frac{c}{\left[f_c^{n-1}(c) \right]^2} \right]^{\frac{1}{2^n}} \tag{1}$$

where c is the complex coordinate of a point outside $\mathcal{M}$ and $f_c^0(c) = c$, $f_c^1(c) = c^2 + c$, $f_c^2(c) = (c^2 + c)^2 + c$ ... are the iterates of $f_c(z) = z^2 + c$ from the initial value $z_0 = 0$. The potential of c is $\log|\Phi(c)|$ and the external argument of c is $\arg\Phi(c)$ [2]. All the points of an external ray have the same external argument. All the points with the same potential define an equipotential line. The external rays are perpendicular to the equipotential lines.

The IEEE 754 Standard for Floating-Point Arithmetic [5] is the most widely-used standard for floating-point computation, and it is followed by many hardware and software implementations. Many computer languages allow or require that some or all arithmetic be carried out using IEEE 754 formats and operations. The current version is IEEE 754-2008 that includes the original IEEE 754-1985. The resolutions of the three basic formats of this Standard are: $res_{single} = 23$, $res_{double} = 52$ and $res_{quadruple} = 112$, according to the number of bits of the mantissas (see table 1).

As we will see, the drawing of an external ray inside a detail of $\mathcal{M}$ is strongly restricted by the number of bits of the floating-point arithmetic used by the computer program. For this reason, the external rays cannot be drawn in certain details of $\mathcal{M}$ with computer programs [6-8] using the double 64 bits format of the old IEEE 754-1985 Standard. This is not due to a failure of programming but a lack of accuracy of the double 64 bits format.

Table 1. Basic formats in the IEEE 754-2008 Standard.

	Sign	Mantissa	Exponent
Single (32 bits)	1	23	8
Double (64 bits)	1	52	11
Quadruple (128 bits)	1	112	15

We are interested in the drawing of external rays of $\mathcal{M}$ [9-18] and in this paper we will analyze the possibilities of the new quadruple 128 bits format of the IEEE 754-2008 Standard. Unfortunately, as we will see in Section 5, the resolution of the quadruple format is not sufficient in some of the cases, and the same occurs with a hypothetical octuple 256 bits format (not defined yet). To avoid this problem, we will introduce in Section 4 a graphical procedure based on the escape lines [19,20,21] and Bézier curves [22], which allows us the drawing of the external rays of a detail of $\mathcal{M}$ when it is not possible to do it using a computer program based in the Böttcher coordinate and running with the IEEE 754 Standard.

2. Tools to calculate external arguments

2.1. Binary expansions

As is known, there are several hyperbolic components of the same period p in $\mathcal{M}$ [23]. The binary expansion of the external argument θ_p of an external ray landing at the root point of a period-p hyperbolic component is period-p periodic and the external argument is rational with odd denominator [2,24]

$$\theta_p = 0.\overline{a_1 a_2 \dots a_p} = \frac{a}{2^p - 1} . \tag{2}$$

In this equation $a_1 a_2 \dots a_p$ are base$_2$ digits such that $a_1 a_2 \dots a_p = a$. For instance, the binary expansion of the external argument $1/5 = 3/(2^4 - 1)$, with $a = 3$ and $p = 4$, is $0.\overline{0011} = 0.00110011\dots$, and the corresponding external ray lands at a period-4 hyperbolic component (see figure 1, where the external rays are drawn with a computer program using the double format of IEEE 754 [6]).

The binary expansion of the external argument $\theta_{n,m}$ of an external ray landing at a Misiurewicz point of $\mathcal{M}$, i.e. a preperiodic point by iteration, is preperiodic of preperiod-n and period-m. Besides, the external argument is rational with even denominator

$$\theta_{n,m} = 0.b_1 b_2 \ldots b_n \overline{a_1 a_2 \ldots a_m} = \frac{a + b(2^m - 1)}{2^n (2^m - 1)} . \tag{3}$$

Here $a_1 a_2 \ldots a_m$ and $b_1 b_2 \ldots b_n$ are base$_2$ digits such that $a_1 a_2 \ldots a_m = a$ and $b_1 b_2 \ldots b_n = b$. For instance, the binary expansion of the external argument $1/6 = 1/2(2^2 - 1)$ (with $a = 1$, $b = 0$, $n = 1$ and $m = 2$) is $0.0\overline{01}$ (see figure 1).
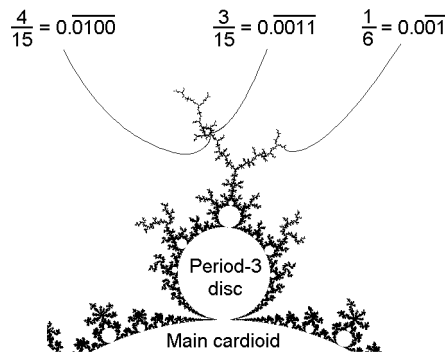

Figure 1. Examples of external arguments of external rays landing at a hyperbolic component and a Misiurewicz point. The figure is drawn using a computer program working with the double format of IEEE 754 Standard [6].

2.2 Rotation number

Devaney [25] associates a rational number p/q to each primary disc c of the Mandelbrot set (a primary disc is directly attached to the main cardioid of the set). The denominator q is the period of the disc. The value of p is fixed by seeing the regions of the Julia set of c when we superimpose the attracting cycle of $f_c(z)$ on the Julia set. The point 0 of the attracting cycle lies in the largest of these regions and the smallest is located exactly p/q revolutions about in the counterclockwise direction. For instance, in figure 2 we can see that $p = 2$ and $q = 5$ in the disc $c = -0.50 + 0.56\mathrm{i}$.

We would like to note that in our papers (see for example [14]) normally we write the rotation number as q/p instead of p/q in order to denominate the period with a p.
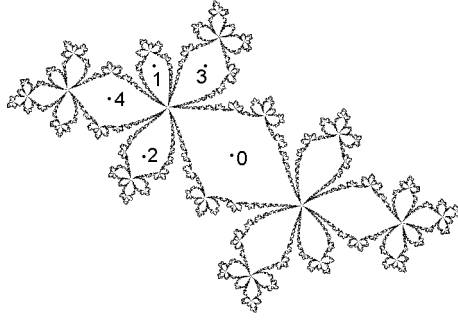
Figure 2. Julia set of $-0.50 + 0.56i$ showing the jumps in the iterative process $f_c(z) = z^2 + c$.

2.3. Tuning algorithm

This algorithm is due to Douady [2]. Let W be a hyperbolic component of period p_1 with centre c_0, and W_0 the main cardioid of $\mathcal{M}$ with period 1 and centre 0. There is a continuous injection $\psi_W : \mathcal{M} \to \mathcal{M}$ such that $c_0 = \psi_W(0)$ and $W = \psi_W(W_0)$. Let us suppose the binary expansions of the external arguments of the external rays landing at the root point of W are $\left(\theta_{p_1}^-, \theta_{p_1}^+\right) = \left(0.\overline{u_1 u_2 \ldots u_{p_1}}, 0.\overline{v_1 v_2 \ldots v_{p_1}}\right)$. Let x be a landing point on W_0 of period p_2 and $x' = \psi_W(x)$ the landing point on W, of period $p_1 p_2$ that Douady called "c_0 tuned by x". If the binary expansions of the external arguments of the external rays landing at x are $\left(\theta_{p_2}^-, \theta_{p_2}^+\right) = \left(0.\overline{s_1 s_2 \ldots s_{p_2}}, 0.\overline{t_1 t_2 \ldots t_{p_2}}\right)$, the corresponding external rays landing at x' have external arguments whose binary expansions can be obtained by substituting each bit of $\left(\theta_{p_2}^-, \theta_{p_2}^+\right)$ by $u_1 u_2 \ldots u_{p_1}$ if the bit is 0 or by $v_1 v_2 \ldots v_{p_1}$ if the bit is 1.

For instance, let us consider the period-4 hyperbolic component with root point located at $-0.15471 + 1.03104i$. The binary expansions of the external arguments of the external rays landing at this point are $\left(\theta_4^-, \theta_4^+\right) = \left(0.\overline{0011}, 0.\overline{0100}\right)$. Let $x = 0.35675 + 0.32861i$ be the root point of a period-5 disc on the main cardioid and $\left(\theta_5^-, \theta_5^+\right) = \left(0.\overline{00001}, 0.\overline{00010}\right)$ the binary expansions of the external arguments of the external rays landing at this point. The corresponding binary expansions of the external arguments of the rays landing at $x' = -0.15255 + 1.03294i$ are

$$\left(\theta_{20}^-, \theta_{20}^+\right) = \left(0.\overline{00110011001100110100}, 0.\overline{00110011001101000011}\right).$$

2.4. Narrow hyperbolic component

A period-p hyperbolic component of the Mandelbrot set is narrow if it contains no component of equal or lesser period in its wake [26]. Then, the external arguments $\left(a^-/(2^p-1),\ a^+/(2^p-1)\right)$ of the external rays landing at the root point of a period-p narrow hyperbolic component differ by $1/(2^p-1)$, because $a^+ - a^- = 1$. For instance, the binary expansions $\left(\theta_4^-,\ \theta_4^+\right) = \left(0.\overline{0011},\ 0.\overline{0100}\right)$, see figure 1, correspond to a narrow period-4 hyperbolic component.

It is obvious that we need a computer program with precision $prec = 2^{-res}$ better than $1/(2^p-1) \simeq 2^{-p}$ to be able to draw separately the two external rays of a period-p narrow hyperbolic component near to its landing point. Taking into account the resolutions of the formats of the IEEE 754-2008 Standard (see table 1), the drawing of the two external rays of a narrow hyperbolic component is impossible when its period is greater than 23, 52 or 112 and we use a single, double or quadruple format respectively.

2.5. Schleicher's algorithm

The Schleicher's algorithm allows us to find the binary expansions of the external arguments of the two external rays landing at the largest disc between two given with rotation numbers p_1/q_1 and p_2/q_2, when the binary expansions of the external rays landing at these discs are known (a detailed description of the algorithm can be seen in [27]).

First, we determine the rotation number of the largest disc by Farey addition [28], i.e. $\left(p_1/q_1\right) \oplus \left(p_2/q_2\right) = \left(p_1 + p_2\right)/\left(q_1 + q_2\right)$. Second, we assume that the binary expansions of the two external rays closest to the $(p_1 + p_2)/(q_1 + q_2)$ disc are known and they are $0.\overline{u_1 u_2 \ldots u_{q_1}}$ and $0.\overline{v_1 v_2 \ldots v_{q_2}}$ such that $0.\overline{u_1 u_2 \ldots u_{q_1}} < 0.\overline{v_1 v_2 \ldots v_{q_2}}$. Third, the binary expansions of the external rays landing at the $(p_1 + p_2)/(q_1 + q_2)$ disc are $\left(0.\overline{u_1 u_2 \ldots u_{q_1} v_1 v_2 \ldots v_{q_2}},\right.$ $\left. 0.\overline{v_1 v_2 \ldots v_{q_2} u_1 u_2 \ldots u_{q_1}}\right)$.

For instance, the higher external argument of the disc with rotation number $\frac{1}{3}$ is $0.\overline{010}$ and the smaller external argument of the disc with rotation number $\frac{2}{5}$ is $0.\overline{01001}$. The biggest disc between the two former ones has rotation number $\frac{1}{3} \oplus \frac{2}{5} = \frac{3}{8}$ and external arguments $\left(0.\overline{01001001},\ 0.\overline{01001010}\right)$.

2.6. Binary expansions in multiple-spiral medallions

As is known, $\mathcal{M}$ contains small copies of itself (babies Mandelbrot sets, BMSs) which in turn contain smaller copies of $\mathcal{M}$, and so on ad infinitum. But the $\mathcal{M}$ set is not self-similar. Actually, every BMS has its own pattern of external decorations. Some of these decorations are called cauliflowers [29], embedded Julia sets [30], or multiple-spiral medallions [11].

Using the symbolic binary expansion, it has been conjectured [11] that the pair of binary expansions of the external arguments of the external rays landing at the cusp of the cardioid of the central BMS in a multiple-spiral medallion $\left(0.\overline{b_1},\ 0.\overline{b_2}\right)$ can be written starting from the binary expansions of its parent $\left(0.\overline{p_1},\ 0.\overline{p_2}\right)$ and its gene $\left(0.\overline{g_1},\ 0.\overline{g_2}\right)$ in the form $0.\overline{b_*} = .\overline{p_* p_* \dots p_* g_*}$ (where b_* is b_1 or b_2, p_* is p_1 or p_2 and g_* is g_1 or g_2). The binary expansions $\left(0.\overline{\beta_1},\ 0.\overline{\beta_2}\right)$ of a non-central BMS has the form $0.\overline{\beta_*} = 0.\overline{b_* \underbrace{p_* p_* \dots p_*}_{j}}$ (where β_* is β_1 or β_2 and j is the level of the BMS [15]). In figure 3 we can see examples of multiple-spiral medallions, where the BMSs until the third level are shown.
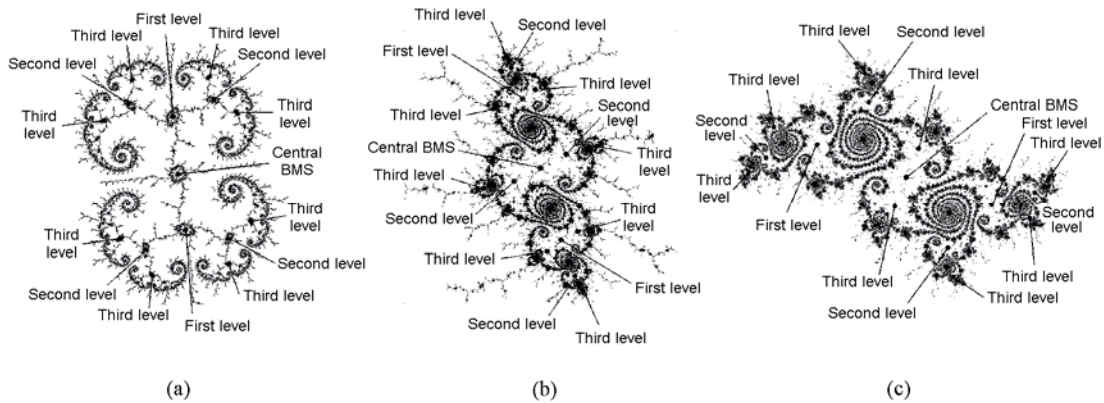

Figure 3. Examples of multiple-spiral medallions [13] in the Mandelbrot set showing the first, second and third levels of BMSs. (a) Single-spiral medallion $-0.1543869 + 1.0308295i$. (b) Double-spiral medallion $-0.16111880 + 1.03632203i$. (c) Triple-spiral medallion $-0.15403780 + 1.03692215i$.

3. The end point of the drawing of an external ray

When we draw an external ray by means of a computer program using the Böttcher coordinate, we observe that the drawing of the ray is interrupted when it comes close to the landing point, i.e., the drawing of an external ray has an end point. This limitation is due to a lack of resolution

of the drawing program that usually works with the floating-point arithmetic of the IEEE 754 Standard.
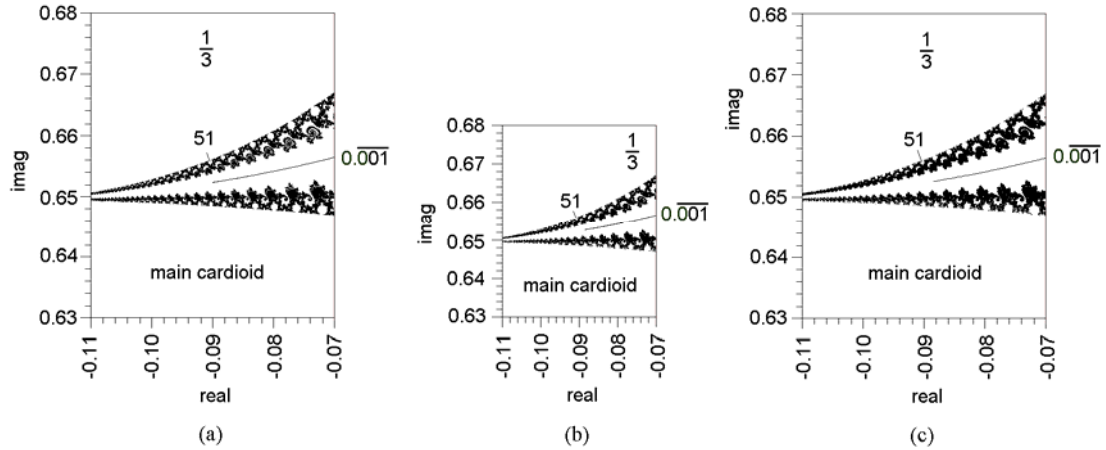

Figure 4. End point of the drawing of the external ray $0.\overline{001}$ obtained with three different programs working with the double format of IEEE 754 Standard. (a) Chéritat's program [6]. (b) Kawahira's program [7]. (c) Jung's program [8].

As an example, in figure 4 we can see the drawing of the external ray $\theta_3^- = 1/7 = 0.\overline{001}$ near the tangent point of the disc of rotation number $\frac{1}{3}$ with the main cardioid, starting from the programs of Chéritat [6], Kawahira [7] and Jung [8]. As far as we know, these programs use the double format of the IEEE 754 Standard with $res_{\text{double}} = 52$. The end point of the drawing of the external ray $0.\overline{001}$ is approximately at $-0.088 + 0.652\,i$, beneath of the period-51 disc. Therefore, we can assume that the end point of the drawing of an external ray occurs when the discs of its vicinity have periods about the number of bits of the mantissa of the format of the IEEE 754.
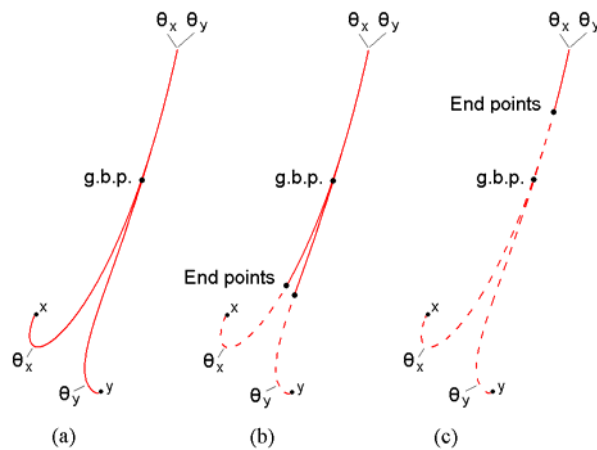
Let us consider the drawing of two close external rays θ_x and θ_y landing at points x and y (see figure 5). If the program has $res = \infty$ as in (a), away from points x and y the two external rays go together in the same pixels until the graphical bifurcation point g.b.p. where they begin to separate. Finally, the landing points x and y would be reached. However, when we use a program with an IEEE 754 format, with finite resolution, the landing points cannot be reached, and there are two cases. When $\left|\theta_x - \theta_y\right| > 2^{-res}$, see (b), the end points appear after reaching the g.b.p. When $\left|\theta_x - \theta_y\right| < 2^{-res}$, see (c), the end points appear before reaching the g.b.p.

4. Drawing external rays when the resolution of the IEEE 754 is not sufficient

When the number of bits of the period (or the sum of the number of bits of the preperiod and period) of the binary expansion of the external argument of an external ray is greater than the number of bits of the quadruple format of the IEEE 754 Standard, obviously is impossible the drawing of the external ray near the landing point by means of a computer program running with this Standard. In this case we operate as follows (see figure 6, where we obtain the same external rays that in figure 1).
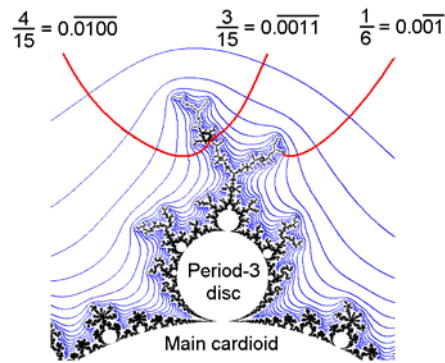

Figure 6. Reproduction of figure 1 according to Section 4.

First, we draw the detail of the Mandelbrot set with escape lines (blue colour in figure 6) [19-21]. The equation of an escape line is $\mathrm{mod}\left[f_c^n(c)\right] = r_e$, where $r_e \geq 2$ is the escape radius and $f_c^0 = c$, $f_c^1 = c^2 + c$, $f_c^2 = (c^2 + c)^2 + c \ldots$. For $n = 0, 1, 2 \ldots$ we have the different escape lines. The escape lines are closed curves that have a clear physical meaning: a point c out of the escape line n but inside the escape line $n - 1$ need n iterations to leave the circle of radius r_e

(i.e., to escape to infinity). Hence, the escape line ∞ is the boundary of the Mandelbrot set. As is well known, if the escape radius is large compared to the size of the set (for instance $r_e = 10^5$) the escape lines can be considered as equipotential lines. The escape lines are obtained as a consequence of the iteration process in the drawing of the detail of the Mandelbrot set and they do not need to be obtained with the Böttcher coordinate.

Second, we draw manually the external rays by means of Bézier curves (red colour in figure 6) [22] starting from the landing points of the external rays in such a way that they are perpendicular to the escape lines.

5. The drawing of the external rays requires great computer resolution

The figure 7 shows a region of the Mandelbrot set near the tangent point of the disc of rotation number $\frac{1}{3}$ with the main cardioid. Between the abscises -0.1184 and -0.1178 there are 1163 pixels and therefore the distance between two consecutive pixels is $d = (0.1184 - 0.1178)/1163 = 5.1 \times 10^{-7}$. The figure has been drawn by means of a program using the IEEE 754 double format where $2^{-res_{double}} = 2^{-52} \simeq 2.2 \times 10^{-16} << d$, with escape lines (in blue colour) and Bézier curves (in red colour) according to Section 4. As we can see next, it is not possible to draw the external rays in this figure by means of a computer program using the Bötcher coordinate, due to a lack of resolution of the quadruple format of the IEEE 754 Standard.
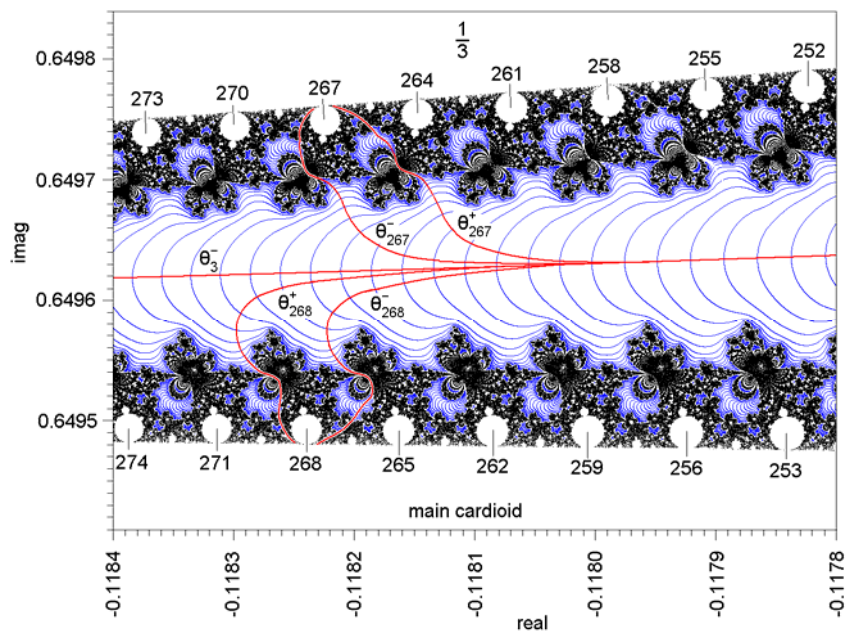

Figure 7. Detail of the Mandelbrot set near the tangent point of the disc with rotation number $\frac{1}{3}$.

In the upper part of the figure 7, there are discs with periods 3×84, 3×85, ... , 3×91, attached to the disc $\frac{1}{3}$. For example, the external arguments of the external rays landing at the tangent point of the disc with period $3\times89=267$ can be obtained by tuning and they are $\left(\theta_{267}^-,\ \theta_{267}^+\right)=\left(0.\overline{\overline{001}^{88}010},\ 0.\overline{\overline{001}^{87}010001}\right)$. Note that the first 262 digits of θ_{267}^- and θ_{267}^+ are the same. Therefore, to be able to draw these external rays separately near the landing point, the resolution of the computer program must be greater than 262. Obviously, this resolution exceeds the possibilities of the quadruple format (128 bits) of the IEEE 754 Standard.

In the lower part of the figure 7 there are discs with periods $3\times83+4$, $3\times84+4$, ... , $3\times90+4$ attached to the main cardioid. The external arguments of the external rays landing at the tangent point of the disc with period $3\times88+4=268$ can be obtained by the Schleicher's algorithm and they are $\left(\theta_{268}^-,\ \theta_{268}^+\right)=\left(0.\overline{\overline{001}^{88}0001},\ 0.\overline{\overline{001}^{88}0010}\right)$. Note that this disc is narrow.

The first 266 digits of θ_{268}^- and θ_{268}^+ are the same and, again, the external rays θ_{268}^- and θ_{268}^+ of figure 7 cannot be drawn separately with a computer program using the quadruple format (neither with the octuple format that it is not defined yet).

Taking into account that $\theta_{267}^+>\theta_{267}^->\theta_3^->\theta_{268}^+>\theta_{268}^-$, the external ray θ_3^- is between rays that cannot be drawn. We conclude that the external ray θ_3^- of figure 7 can not be drawn by a computer program using the quadruple format of IEEE 754. In this case, we propose the drawing of the external rays according to Section 4.

We have shown an example where the double format of IEEE 754 Standard can draw a detail of the Mandelbrot set but the quadruple format (more précis) cannot draw the external rays in the detail. Hence, the drawing of the external rays in a region of the Mandelbrot set needs greater computer resolution than the drawing of the detail itself.

5.1. Example.

Let us consider the double-spiral medallion [13,15] located at $-0.16111880+1.03632203i$. The figure 8 shows the location of the medallion and in figure 8(a) we can see his parent $\left(0.\overline{p_1},\ 0.\overline{p_2}\right)=\left(0.\overline{0011},\ 0.\overline{0100}\right)$ and his gene $\left(0.\overline{g_1},\ 0.\overline{g_2}\right)=\left(0.\overline{001},\ 0.\overline{010}\right)$ [9,11].

The figure 9 shows the medallion in detail with escape lines (in blue colour) and external rays (in red colour) according to Section 4. As is known [15], the binary expansions of the external arguments of the external rays landing at the cusp of the central BMS of a double-spiral

medallion have symbolic binary expansions $\left(0.\overline{b_1}, \ 0.\overline{b_2}\right) = \left(0.\overline{\overline{p_1 p_2}^{\,i} p_1 p_1 g_2}, \ 0.\overline{\overline{p_1 p_2}^{\,i+1} g_1}\right)$ with

$i = 1, 2, 3 \dots$. In the medallion of figure 9 we have $i = 32$ and

$$\left(0.\overline{b_1}, \ 0.\overline{b_2}\right) = \left(0.\overline{\overline{00110100}^{\,32} 00110011010}, \ 0.\overline{\overline{00110100}^{\,33} 001}\right).$$

Therefore the period of the central BMS is 267, as we easily can verify by direct iteration of $-0.16111880 + 1.03632203i$. Note that the first 261 bits of the pair $\left(0.\overline{b_1}, \ 0.\overline{b_2}\right)$ are the same.
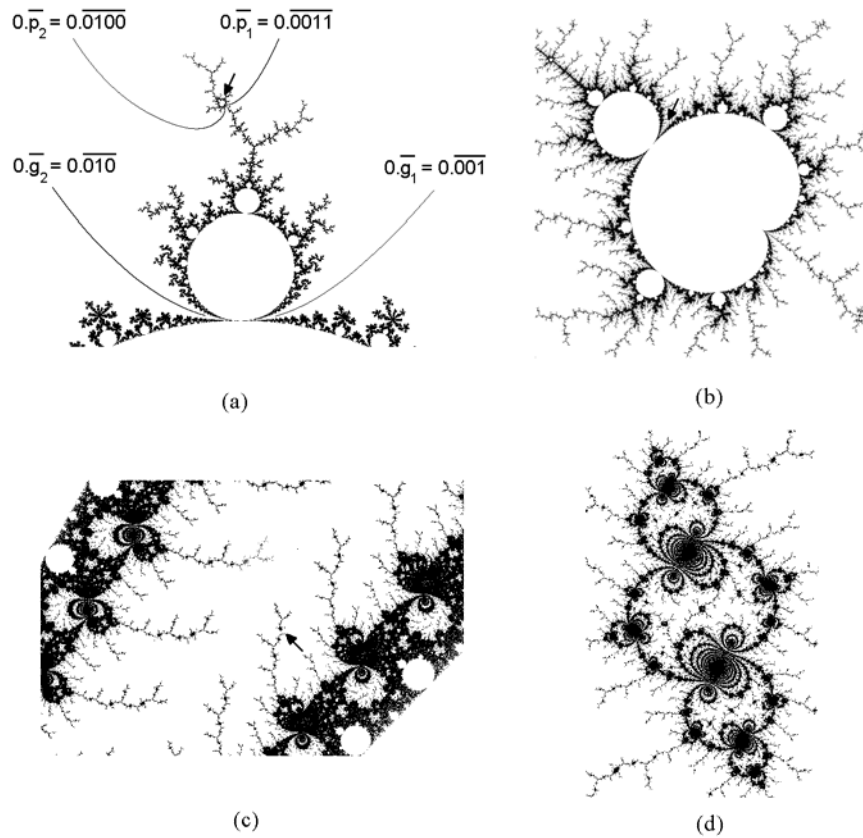

Figure 8. Successive magnifications to locating the double-spiral medallion centred at $-0.16111880 + 1.03632203i$ (the medallion is marked by the arrow). (a) The parent $\left(0.\overline{p_1}, \ 0.\overline{p_2}\right) = \left(0.\overline{0011}, \ 0.\overline{0100}\right)$ in the wake of the gene $\left(0.\overline{g_1}, \ 0.\overline{g_2}\right) = \left(0.\overline{001}, \ 0.\overline{010}\right)$. (b) The period-4 parent. (c) The valley between the period-(2×4) disc of the parent and the cardioid of the parent. (d) The medallion.

The medallion has two principal tips. One of them can be obtained as the limit of the BMSs $\left(0.\overline{b_1 p_2}, \ 0.\overline{b_2 p_1}\right), \ \left(0.\overline{b_1 p_2 p_2}, \ 0.\overline{b_2 p_1 p_1}\right), \ \left(0.\overline{b_1 p_2 p_2 p_2}, \ 0.\overline{b_2 p_1 p_1 p_1}\right) \dots$ and it is

$$\left(0.\overline{b_1 \, \overline{p_2}}, \ 0.\overline{b_2 \, \overline{p_1}}\right) = \left(0.\overline{00110100}^{\,32} 001100110100\overline{0100}, \ 0.\overline{00110100}^{\,33} 0010\overline{0011}\right).$$

Analogously, the other principal tip is

$$\left(0.b_1\overline{p_1},\ 0.b_2\overline{p_2}\right) = \left(0.\overline{00110100}^{\,32}001100110100\overline{011},\ 0.\overline{00110100}^{\,33}001\overline{0100}\right).$$

The two tips have preperiods 267 and periods 4. Also note that the first 261 bits of the pairs $\left(0.b_1\overline{p_2},\ 0.b_2\overline{p_1}\right)$ and $\left(0.b_1\overline{p_1},\ 0.b_2\overline{p_2}\right)$ are the same.

It is evident that each one of the binary expansions of the external arguments of the BMSs and Misiurewicz points in this medallion must be in the interval $\left[0.b_1\overline{p_1},\ 0.b_2\overline{p_2}\right]$ where the first 261 bits of the binary expansions are the same. We deduce that it is not possible to draw none of the external rays inside of this medallion using a computer program working with the quadruple format (128 bits) of IEEE 754 Standard, nor with the octuple format (256 bits, not yet defined).

However it is possible to draw the external rays of the medallion according to Section 4. In figure 9 we can see the external rays landing at the central BMS $\left(0.\overline{b_1},\ 0.\overline{b_2}\right)$, the tips $\left(0.b_1\overline{p_2},\ 0.b_2\overline{p_1}\right)$ and $\left(0.b_1\overline{p_1},\ 0.b_2\overline{p_2}\right)$, the two BMSs of the first level, the four BMSs of the second level and the eight BMSs of the third level.

Figure 9. Double-spiral medallion located at $-0.16111880 + 1.03632203i$ showing escape lines (blue colour) and Bézier curves (red colour) according to Section 4.

6. Conclusions

It has been shown that the drawing of the external rays in a detail of the Mandelbrot set, using a computer program starting from the Böttcher coordinate and running with the current IEEE 754 Standard for Floating-Point Arithmetic, requires more resolution than the drawing of the detail itself. For this cause, in certain details of the Mandelbrot set obtained with the quadruple format of this Standard (the more précis), it is not possible to draw the external rays due to a lack of resolution. In these cases we have introduced a method based on escape lines and Bézier curves, which allows the drawing of the external rays.

References

[1] Douady A, Hubbard J H 1982 Itération des polynômes quadratiques complexes. *C. R. Acad. Sci. Paris Sér. I Math.* **294** 123–6

[2] Douady A 1986 Algorithms for computing angles in the Mandelbrot set. *Chaotic Dynamics and Fractals* Barnsley M, Demko S G (Eds.), Academic Press, New York 155-68

[3] Douady A 1986 Julia set and the Mandelbrot set. *The Beauty of Fractals* Peitgen H O, Richter P H (Eds.), Springer, Berlin 161–73

[4] Carleson L and Gamelin T W 1993 *Complex Dynamics*, Springer, Berlin

[5] IEEE 754-2008 Standard for Floating-Point Arithmetic
http://ieeexplore.ieee.org/xpl/freeabs_all.jsp?arnumber=4610935

[6] Chéritat A 1999 Dynamique Holomorphe
http://www.math.univ-toulouse.fr/~cheritat/

[7] Kawahira T 2008 Mandel
http://www.math.nagoya-u.ac.jp/~kawahira/programs/mandel.html

[8] Jung W 2012 Mandel: software for real and complex dynamics
http://www.mndynamics.com/indexp.html

[9] Romera M, Pastor G, Álvarez G and Montoya F 2004 External arguments of Douady cauliflowers in the Mandelbrot set. *Comput. Graph.* **28** 437-49

[10] Pastor G, Romera M, Álvarez G and Montoya F 2002 Operating with external arguments in the Mandelbrot set antenna. *Physica* D **171** 52-71

[11] Romera M, Pastor G, Álvarez G and Montoya F 2006 External arguments in the multiple-spiral medallions of the Mandelbrot set. *Comput. Graph.* **30** 461-70

[12] Pastor G, Romera M, Álvarez G and Montoya F 2005, External arguments for the chaotic bands calculation in the Mandelbrot set. *Physica* A **353** 145-58

[13] Romera M, Álvarez G, Arroyo D, Orue A B, Fernandez V and Pastor G 2008 Drawing and computing external rays in the multiple-spiral medallions of the Mandelbrot set. *Comput. Graph.* **32** 597-610

[14] Pastor G, Romera M, Álvarez G, Arroyo D and Montoya F 2006 Equivalence between subshrubs and chaotic bands in the Mandelbrot Set. *Discrete Dyn. Nat. Soc.* Article ID 70471, 25 pages

[15] Romera M, Pastor G, Orue A B, Arroyo D and Montoya F 2009 Coupling patterns of external arguments in the multiple-spiral medallions of the Mandelbrot set. *Discrete Dyn. Nat. Soc.* Article ID 135637, 14 pages

[16] Pastor G, Romera M, Álvarez G, Nunez J, Arroyo D and Montoya F 2007 Operating with external arguments of Douady and Hubbard. *Discrete Dyn. Nat. Soc.* Article ID 45920, 17 pages

[17] Pastor G, Romera M, Álvarez G, Arroyo D, Orue A B, Fernandez V and Montoya F 2008 Algorithm for external arguments calculation of the nodes of a shrub in the Mandelbrot set. *Fractals* **16** 159-68

[18] Pastor G, Romera M, Álvarez G, Arroyo D, Orue A B, Fernández V and Montoya F 2009 A general view of pseudoharmonics and pseudoantiharmonics to calculate external arguments of Douady and Hubbard. *Appl. Math. Comput.* **213** 484-97

[19] Peitgen H.-O. and Richter P. H. 1986 *The Beauty of Fractals* Springer-Verlag, New York 163

[20] Philip K. W. 1992 Field lines in the Mandelbrot set, *Comput. Graph.* **16** 443–7

[21] Romera M, Pastor G and Montoya F 1996 Graphic tools to analyse one-dimensional quadratic maps. *Comput. Graph.* **20** 333-9

[22] Bézier P 1968 Procédé de définition numérique des courbes et surfaces non mathématiques: système Unisurf. *Automatisme* **13** 189-96.

[23] Lutzky M 1988 Counting stable cycles in unimodal iterations. *Phys. Lett.* A **131** 248-50

[24] Branner B 1989 The Mandelbrot set. *Chaos and Fractals: the Mathematics Behind the Computer Graphics*, *Proc. Symp. Appl. Math.* **39** AMS 75-105

[25] Devaney R L 1995 The fractal geometry of the Mandelbrot set 2: How to count and how to add. *Fractals* **3** 629-40

[26]   Schleicher D 2012 Internal addresses of the Mandelbrot set and Galois groups of polynomials. arXiv:math/9411238v3

[27]   Devaney R L 1994 The complex dynamics of quadratic polynomials, *Complex Dynamical Systems* Devaney R L (Ed.), AMS, Cincinnati 1-29

[28]   Farey J 1816 On a curious property of vulgar fractions, *Philos. Mag.* **47** 385-6

[29]   Douady A, Buff X, Devaney R L and Sentenac P 2000 Baby Mandelbrot sets are born in cauliflowers. *The Mandelbrot set, theme and variations* Lei T (Ed.), University Press Cambridge 19-36

[30]   Munafo R P 2008 Embedded Julia set.
       http://mrob.com/pub/muency/embeddedjuliaset.html